Draft version November 18, 2021
Typeset using LaTeX **RNAAS** style in AASTeX631

Measuring Stellar Heartbeats: an Asteroseismic Analysis of KIC7431665

Grace E. Chiodo[1]

[1] *Villanova University, 800 Lancaster Avenue, Villanova, PA 19085, USA*

ABSTRACT

Heartbeat binaries represent a class of red giant stars that receive particular attention in astronomy for their solar-like oscillations. Their light curves exhibit two forms of variability: interior stellar pulsations and binary interaction causing tidal distortions at periastron. Asteroseismology takes advantage of stellar pulsations to probe the interiors of stars that would otherwise be unobservable. In this study, we conduct a detailed asteroseismic analysis of KIC7431665 from *Kepler* data to determine the fundamental parameters of the system. We find $\nu_{max} = 54.5 \pm 0.4$ μHz and $\Delta\nu = 5.47 \pm 0.01$ μHz for KIC7431665. Applying scaling relations to the ν_{max} and $\Delta\nu$ for KIC7431665 yields the following stellar parameters: R = 9.58 $\pm$ 0.08 $R_\odot$, M = 1.43 $\pm$ 0.03 $M_\odot$, L = 36.2 $\pm$ 0.59 $L_\odot$, and log(g) = 2.63 $\pm$ 0.001 dex. We hope future studies will conduct a binary analysis to confirm the parameters and characterize the oscillation modes.

1. INTRODUCTION

One success of NASA's *Kepler* Space Telescope (2009-2018) stems from the discovery of red giant heartbeat stars. Heartbeat stars are a class of highly eccentric binary stars with light curves that clearly depict strong gravitational distortion and heating at periastron Themeßl et al. (2018). This discovery presents an opportunity for asteroseismic analyses on the structure of the new stellar class by studying the high-resolution observations in the *Kepler* field of view. A heartbeat star can be further classified based on the type of stars within the system (Beck et al. (2014)). Heartbeat red giant binaries, for example, consist of a red giant and a binary companion (Bedding & Kjeldsen (2010)). A red giant star contains a helium core with a hydrogen-burning shell surrounded by a convective envelope (LeBlanc (2010)). An asteroseismic analyses of solar-like oscillations in the exterior layers of the red giant determines the fundamental parameters and the details of the internal structure of the heartbeat binary.

The convective envelope drives the oscillations of heartbeat red giants (Themeßl et al. (2018)). Convection in the envelope generates solar-like oscillations via the movement of plasma that transports energy and dampens oscillations (Bedding & Kjeldsen (2003)).The oscillations get amplified in heartbeat stars due to the highly eccentric orbit. A distinguishing feature of heartbeat red giants is that an oscillation pattern extends across all inclinations in the light curve, rather than the narrow range of the eclipse (Beck et al. (2014)). This allows more extensive measurements of binary characteristics compared to other types of binary stars.

The mode of each oscillation depends on the restoring force. Pressure (p) modes cause radial motion due to the pressure gradient, while gravity (g) modes cause transverse motion due to buoyancy (Bedding et al. (2011)). In the case of red giants, p modes dominate the solar-like oscillations in the convective envelope while g modes have the largest amplitudes in the core. The non-radial modes of oscillation continuously work to restore a star to its equilibrium configuration. The trajectory of a wave inside a star deviates from the radial symmetry found in an approximately spherical object. The oscillating behavior generates repeated variations in the radiation observed from variable stars as the star continuously attempts to return to its equilibrium form (LeBlanc (2010)). These variations receive detailed study in the field of asteroseismology because they reflect the internal processes of a star that would otherwise be unobservable.

The fundamental properties obtained in asteroseismic analyses derive from various scaling relations. The scaling relations for stellar mass and radius depend on the pulsation frequencies and largest separation frequency from the power spectrum. The relations also depend on the surface temperature because the temperature determines the oscillation mechanism of a star (Bedding & Kjeldsen (2003)). Huber et al. (2012) presents a comparison of the fundamental properties determined with asteroseismic scaling relations to those determined from near-model-independent methods. The comparison shows good agreement between the two methods, which confirms the accuracy of fundamental pa-

Parameter	Value	Reference
Radius	$9.4 \pm 0.1\ R_\odot$	1
Mass	$1.39 \pm 0.05\ M_\odot$	1
Log(g)	2.62	1
T_{eff}	4580 K	1
Distance	$939.952^{+13.873}_{-13.474}$ pc	2
Mean g magnitude	10.94894	2

Table 1. Reference 1: Beck et al. (2014); Reference 2: Brown et al. (2021).

rameters obtained with asteroseismic techniques. The scaling relations remain the preliminary method of extracting parameters from stellar pulsations (e.g. Hon et al. (2020); De Moura et al. (2020); Zhang et al. (2020)). Moreover, the scaling relations provide a reliable method of determining fundamental properties of heartbeat red giants and other stars that exhibit solar-like oscillations.

The preliminary studies of the fundamental properties of heartbeat red giants involved statistical analyses of large data sets. Beck et al. (2014) conducted an asteroseismic study of 18 eccentric binaries with *Kepler* data. The sample included the heartbeat binary KIC7431665. The results from the study include a mass of $1.39 \pm 0.05\ M_\odot$ and a radius of $9.4 \pm 0.1\ R_\odot$ for KIC7431665. Table 1 details the parameters from the study. These parameters effectively reflect the red giant alone rather than an average of the binary companions due to the large size of the red giant. The red giant dominates the observational properties of a heartbeat binary unless the companion star is of high density, such as a white dwarf. The high resolution of the observations from the *Kepler* mission allows for more extensive asteroseismic analyses of red giant binaries Cherinka et al. (2019).

The following study presents a detailed asteroseismic analysis of the heartbeat red giant KIC7431665 using *Kepler* data. Section 2 details the observations performed from the *Kepler* mission. Section 3 outlines the analysis of this data with the methods of obtaining stellar parameters from the light curve and power spectrum. Section 4 discusses the significance of the study and the next step for future ones. In Section 5, we reflect on the results of the study and the importance of obtaining stellar parameters.

2. OBSERVATIONS

The observations for KIC7431665 covers Q0-Q17 of long cadence *Kepler* data from 2009 to 2013. The Kepler Input Catalog (KIC) contains one ephemeris for this data with a period of 281.4 ± 0.0028 days. The long cadence has 6.02 second exposures and 0.52 second readout times. This yields 29.4 minute observations by integrations over 270 exposures Gilliland et al. (2010). We generate light curves of the *Kepler* photometric observations from the photometric flux data already compiled in the catalog. The effective temperature applied in this study is 4580 K from the results of Beck et al. (2014) analyzing *Kepler* data (Q0-Q14).

3. SEISMIC ANALYSIS

3.1. Stellar Parameters

The photometric data from *Kepler* provides the normalized flux with corresponding BKJD days to generate light curves. We combine the individual light curves from Q0-Q17 to produce a light curve spanning across all observation windows. The light curve contains large variations due to the highly eccentric orbit of the binary companions. These variations introduce error in frequency analyses by suggesting false oscillations of the star. We remove these eclipses by winsorization of all normalized flux values above 1.0015 or below 0.9985 to reduce flux variations unrelated to the solar-like oscillations.

The light curve must be converted to a power spectrum to locate the region of excess power, which contains the signatures of the solar-like oscillation modes. The LIGHTKURVE package includes the Lomb-Scargle method as a built-in function to construct a periodogram from light curve data. *Figure 2* displays the power density spectrum for KIC7431665. We normalize the power and zoom in on the region of excess power (30-80 μHz). A Gaussian fit approximates the mode envelope containing the oscillation modes (see *Fig. 3*). The mode envelope contains the frequency information necessary to calculate stellar parameters from scaling relations. The spikes in power in this region correspond to modes of oscillation. Equal frequency intervals separate modes of the same radial order (ie. radial or dipole modes).

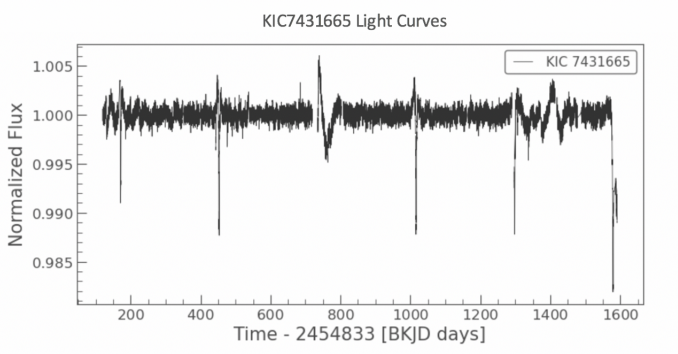

Figure 1. The light curve combines Q0-Q17 *Kepler* observations of KIC7431665. The large drops in the normalized flux correspond to eclipses of the binary companions.

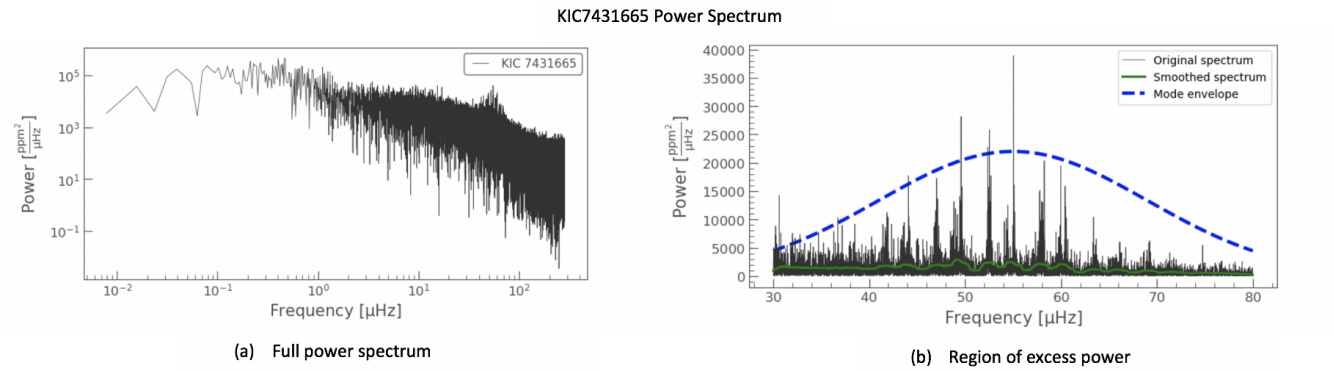

Figure 2. The figure contains the power spectral density of the *Kepler* light curve of KIC7431665. *Figure 2a* includes the entire power spectrum, and *Figure 2b* focuses on the region of power excess. The region of excess power has a Gaussian fit for the mode envelope and a smoothed spectrum (filter width = 7 days) overlayed on the data.

The initial power spectral density data contains noise from the convective background and tidally-induced flux modulations from the heartbeat event. We remove this noise by flattening the power spectrum with a triangular filter (filter width = 7 days). The triangular method applies a boxcar filter to another boxcar. We then obtain the peak frequency of the excess of oscillation power ν_{max} by running a two-dimensional autocorrelation function on the flattened power spectrum. The autocorrelation function for red giant branch stars in the LIGHTKURVE package shifts windows of 25 μHz along the data to evaluate the correlation of the data with itself. The package then calculates the mean collapsed correlation of the two-dimensional autocorrelation function results to determine the frequency with the highest correlation power. The frequency associated with the peak of a one-dimensional Gaussian fit to the mean collapsed correlation yields the value of ν_{max}. We find that the *Kepler* data for KIC7431665 has $\nu_{max} = 54.50 \pm 0.4$ μHz. The uncertainty range results from a boostrapping analysis of the *Lightcurve* methods (see *Section 3.2*).

The result for ν_{max} becomes an essential parameter in the calculation for $\Delta\nu$. The LIGHTKURVE package determines $\Delta\nu$ by evaluating one full-width-half-max window on either side of ν_{max} in the power spectrum. This ensures that the window includes all visible oscillation modes. We find $\Delta\nu = 5.47 \pm 0.01$ μHz for KIC7431665 (see *Section 3.2* for the calculation of the uncertainty range). We then calculate the mass, radius, and luminosity for KIC7431665 with the following scaling relations:

where $R_\odot$, $M_\odot$, $L_\odot$, and $T_{eff}^\odot$ represent the solar radius, mass, luminosity, and effective temperature, respectively. We adopt solar values of ν_{max} and $\Delta\nu$ from Huber et al. (2011) and the solar effective temperature from Prša et al. (2016). The scaling relations yield the following parameters: R = 9.58 $\pm$ 0.08 $R_\odot$, M = 1.43 $\pm$ 0.03 $M_\odot$, and L = 36.2 $\pm$ 0.59 $L_\odot$. The bootstrapping analysis provided uncertainty ranges for the frequency values ν_{max} and $\Delta\nu$ which

$$\frac{R_*}{R_\odot} = \frac{\nu_{\rm max}}{\nu_{\rm max}^\odot} \times \left(\frac{\Delta\nu}{\Delta\nu_\odot}\right)^{-2} \times \sqrt{\frac{T_{\rm eff}}{T_{\rm eff}^\odot}}$$

$$\frac{M_*}{M_\odot} = \left(\frac{R_*}{R_\odot}\right)^3 \times \left(\frac{\Delta\nu}{\Delta\nu_\odot}\right)^2$$

$$\frac{L_*}{L_\odot} = \left(\frac{\nu_{\rm max}}{\nu_{\rm max}^\odot}\right)^2 \times \left(\frac{\Delta\nu}{\Delta\nu_\odot}\right)^{-4} \times \left(\frac{T_{\rm eff}}{T_{\rm eff}^\odot}\right)^5$$

we extend to the uncertainties of the stellar parameters with the dependence of the scaling relations on frequency (see *Section 3.2*). A relation for surface gravity stems from the asteroseismic scaling relations as well. We find log(g) = 2.63 ±0.001 dex by applying:

$$g_* = g_\odot + \left(\frac{\nu_{max}}{\nu_{max}^\odot}\right) * \left(\frac{T_{eff}}{T_{eff}^\odot}\right)^{0.5}$$

where $g_\odot$ represents the solar surface gravity, and g_* represents the surface gravity of the target star. We again adopt the solar asteroseismic parameters from Huber et al. (2011) and the solar effective temperature from Prša et al. (2016).

3.2. Uncertainty Determination

The uncertainty ranges result from the standard error and error propagation analyses. We determine the standard error from a bootstrapping resampling process. We consider the light curve data to be the entire population set and then generate a random sample from that data. A function constructs the power spectrum for that sample and calculates ν_{max} and $\Delta\nu$ for the sample using the same LIGHTKURVE code from the initial analysis presented in *Section 3.1*. We then resample the population with 1,000 iterations with each iteration returning the standard deviations and means of the current distributions for ν_{max} and $\Delta\nu$ values. We calculate the uncertainty ranges for ν_{max} and $\Delta\nu$ by dividing the final standard deviations by the square root of number of iterations.

Error propagation applies the uncertainty ranges from the resampling process to the stellar parameters from the LIGHTKURVE results. The error propagation calculations for the scaling relations sum the squares of the propagation of errors for each variable from this study that contains error (ie. ν_{max} and $\Delta\nu$).

3.3. Échelle Diagram

The *Lightcurve* package generates an Échelle diagram of the power spectrum. An Échelle diagram aligns the frequency data in slices of $\Delta\nu$. This creates vertical ridges that correspond to modes of equal radial degree (Bedding & Kjeldsen (2010)). In the Échelle diagram for KIC7431665, we see clear ridges for the oscillation modes (see *Fig. 3*). The diagram indicates oscillation modes of l=1, 2, and 0 corresponding to the ridges from left to right. The strength of the vertical ridges for the frequency mod. 5.47 μHz verifies that we can confidently perform calculations dependent on $\Delta\nu$, such as the scaling relations for stellar parameters.

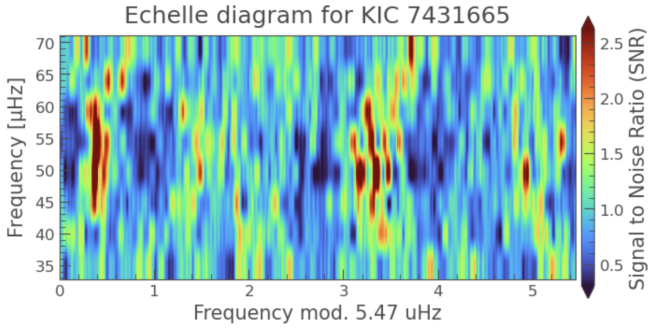

Figure 3. The Échelle diagram illustrates the oscillation modes for KIC7431665. The modes correspond to the vertical ridges with modes l=1, 2, 0 from left to right.

4. DISCUSSION

The seismic analysis of KIC7431665 demonstrates the necessity for single-star studies in refining the results of pipeline projects that instead generalize the methodology to thousands of stars. *Table 2* contains the stellar parameters from this study with a comparison to values from the literature of larger studies. For the comparison to Beck et al. (2014), we find percent differences of 1.24% and 0.16% for ν_{max} and $\Delta\nu$, respectively. For the comparison to Manuel & Hambleton (2018), we find percent differences of 0.92% and 0.18% for ν_{max} and $\Delta\nu$, respectively.

	This work	Beck et al. (2014)	Yu et al, (2018)
ν_{max} (μHz)	54.5 ± 0.4	54.0 ± 0.7	53.83 ± 1.04
$\Delta\nu$ (μHz)	5.47 ± 0.01	5.46 ± 0.02	5.461 ± 0.022
Radius ($R_\odot$)	9.58 ± 0.08	9.4 ± 0.1	9.49 ± 0.2
Mass ($M_\odot$)	1.43 ± 0.03	1.39 ± 0.05	1.14 ± 0.01
Luminosity ($L_\odot$)	36.2 ± 0.59	35 ± 2	35.5 ± 0.6
Log(g) (dex)	2.63 ± 0.001	2.62	2.639 ± 0.010

Table 2. Reference 1: Beck et al. (2014); Reference 2: Yu et al. (2018).

The Échelle diagram reveals the presence of oscillation modes l=1, 2, and 0. This indicates both radial and dipole pulsations contributing to the solar-like oscillations. The mix of radial and non-radial modes confirms the expected behavior of the star, but photometric observations fail to capture all modes of oscillation within a star. A future study should obtain spectroscopic observations of KIC7431665 to detect higher non-radial modes of oscillation.

The fundamental parameters provide an important first step in stellar modeling. A future study of KIC7431665 should conduct a binary analysis to investigate the nature of the flux variations in the observed light curve. A unique feature of heartbeat red giants is that they exhibit two forms of variability: solar-like oscillations and binary interactions. An interesting binary analysis would separate the stellar pulsations from the binary features of the star. The residual pulsation frequencies would then indicate the presence of different types of stellar pulsations. We expect to find tidal pulsations due to the strong tidal forces at periastron, but other studies of heartbeat binaries reveal more interesting causes of pulsations, such as delta Scuti and gamma Doradus Manuel & Hambleton (2018). A binary analysis of KIC7431665 would also confirm the stellar parameters presented in this study.

5. CONCLUSIONS

The asteroseismic study analyses the solar-like oscillations of KIC7431665 to reveal its stellar parameters. The *Kepler Input Catalog* provides detections from the *Kepler* mission for the target. A power spectrum generated from the light curve of the *Kepler* observations depicts clear power excess in the region of the mode envelope. The even spacing between the drops in flux indicates the oscillation modes present for the star. We apply a 2D-autocorrelation function to the region of excess power to determine the frequency of maximum power and the frequency difference between modes of the same radial order. We find $\nu_{max} = 54.5 \pm 0.4$ μHz and $\Delta\nu = 5.47 \pm 0.01$ μHz for KIC7431665. Applying scaling relations to the ν_{max} and $\Delta\nu$ for KIC7431665 yields the following stellar parameters: R = 9.58 ± 0.08 $R_\odot$, M = 1.43 ± 0.03 $M_\odot$, L = 36.2 ± 0.59 $L_\odot$, and log(g) = 2.63 ± 0.001 dex. The uncertainty ranges result from the standard error and error propagation.

An Échelle diagram for KIC7431665 depicts the oscillation modes present in the photometric observations. We find modes of radial order l=1, 2, and 0. This strong vertical ridges formed by applying frequency mod 5.47 μHz provide a further verification of the parameters obtained from this study. As a result of this detailed asteroseismic analysis, we can confidenty apply the stellar parameters for KIC7431665 to future stellar models and binary studies.

ACKNOWLEDGEMENTS

Thank you to Dr. Andrej Prša who assisted in the research process. A special thank you to Dr. Kelly Hambleton who offered expertise in the field of asteroseismology. We acknowledge the funding for the *Kepler* Mission provided by NASA's Science Mission Directorate and the *Kepler* team for the data. We would like the Conor Michael Larsen

and Kevin Brian Moposita for supporting remarks and suggestions throughout the study. Thank you to the team that created LIGHTKURVE and Michael Christian Davis for editing a section of the LIGHTKURVE code for this study.

REFERENCES

Beck, P. G., Hambleton, K., Vos, J., et al. 2014, A&A, 564, A36, doi: 10.1051/0004-6361/201322477

Bedding , T. R., & Kjeldsen, H. 2010, Communications in Asteroseismology, 161, 3, doi: 10.1553/cia161s3

Bedding, T. R., & Kjeldsen, H. 2003, PASA, 20, 203, doi: 10.1071/AS03025

Bedding, T. R., Mosser, B., Huber, D., et al. 2011, Nature, 471, 608, doi: 10.1038/nature09935

Brown, A. G. A., Vallenari, A., Prusti, T., et al. 2021, Astronomy & Astrophysics, 650, doi: 10.1051/0004-6361/202039657e

Cherinka, B., Andrews, B. H., Sánchez-Gallego, J., et al. 2019, The Astronomical Journal, 158, 74, doi: 10.3847/1538-3881/ab2634

De Moura, B. L., Beck, P. G., Di Mauro, M. P., et al. 2020, ApJ, 894, 67, doi: 10.3847/1538-4357/ab80c8

Gilliland, R. L., Jenkins, J. M., Borucki, W. J., et al. 2010, ApJL, 713, L160, doi: 10.1088/2041-8205/713/2/L160

Hon, M., Bellinger, E. P., Hekker, S., Stello, D., & Kuszlewicz, J. S. 2020, MNRAS, 499, 2445, doi: 10.1093/mnras/staa2853

Huber, D., Ireland, M. J., Bedding, T. R., & et al. 2012, ApJ, 760, doi: 10.1088/0004-637X/760/1/32

Huber, D., Bedding, T. R., Stello, D., et al. 2011, ApJ, 743, 143, doi: 10.1088/0004-637X/743/2/143

LeBlanc, F. 2010, An Introduction to Stellar Astrophysics

Manuel, J., & Hambleton, K. 2018, in American Astronomical Society Meeting Abstracts, Vol. 231, American Astronomical Society Meeting Abstracts #231, 146.01

Prša, A., Harmanec, P., Torres, G., et al. 2016, AJ, 152, 41, doi: 10.3847/0004-6256/152/2/41

Themeßl, N., Hekker, S., Southworth, J., et al. 2018, MNRAS, 478, 4669, doi: 10.1093/mnras/sty1113

Yu, J., Huber, D., Bedding, T. R., et al. 2018, VizieR Online Data Catalog, J/ApJS/236/42

Zhang, X., Li, Y., Wu, T., & Su, J. 2020, MNRAS, 494, 511, doi: 10.1093/mnras/staa667